Photoconductive properties of Bi_2S_3 nanowires

J. Andzane[1,a)], G. Kunakova[1], J. Varghese[2,3], J. D. Holmes[2,3], D. Erts[1]

[1]*Institute of Chemical Physics, University of Latvia, Riga, Latvia*

[2]*Materials Chemistry & Analysis Group, Department of Chemistry and the Tyndall National Institute, University College Cork, Cork, Ireland*

[3]*Centre for Research on Adaptive Nanostructures & Nanodevices (CRANN), Trinity College Dublin, Dublin 2, Ireland*

The photoconductive properties of Bi_2S_3 nanowires synthesized inside anodized alumina (AAO) membrane have been characterized as a function of illuminating photon energy between the wavelengths of 500 to 900 nm and at constant illumination intensity of 1-4 $\mu W \cdot cm^{-2}$. Photoconductivity spectra, photocurrent values, photocurrent onset/decay times of individual Bi_2S_3 nanowires liberated from the AAO membrane were determined and compared with those of arrays of as-produced Bi_2S_3 nanowires templated inside pores of AAO membrane. The alumina membrane was found to significantly influence the photoconductive properties of the AAO-hosted Bi_2S_3 nanowires, when compared to liberated from the AAO membrane individual Bi_2S_3 nanowires, possibly due to charge carrier trapping at the interface between the nanowire surface and the pore walls.

I. INTRODUCTION

One-dimensional semiconductor nanomaterials, in the form of nanorods, nanowires, nanotubes and even nanobelts have been successfully utilized as building blocks for numerous nanoelectronic devices[1-7]. One of the most studied properties of nanowires is their sensitivity to light, permitting their use in photovoltaic and photo-detector devices, optical switches and sensors [8-13]. In particular, metal chalcogenides have been widely used in optoelectronic devices [14].

This research details the photoconductive properties of bismuth sulfide (Bi_2S_3) nanowires. Whilst there are a number of reports describing the photoresponsive properties of Bi_2S_3 thin films, nanowires and nanoparticles [15-19], there are no reports detailing photoconductive properties of the individual Bi_2S_3 nanowires as function of the illuminating photon energy at low (μWcm^{-2}) illumination intensities as well as the influence an encasing template, *e.g.* AAO, has on the photoconductive properties of Bi_2S_3 nanowires. Recent investigations of Bi_2S_3 thin films have shown that they exhibit direct band gaps of 1.2 – 2.0 eV respectively, and display a reasonable photosensitivity response, indicating their potential use in optoelectronic devices [16,17]. Bao *et al.* and Xi *et al.* have also demonstrated photoswitchable Bi_2S_3 nanowires and nanowire networks [12,13,20], where the nanowires exhibited a pronounced positive photoconductivity and a millisecond response time upon illumination

with visible light. For most of these studies laser irradiation, with energies between 70-100 $\mu W \cdot cm^{-2}$ [12], or halogen and tungsten filaments were employed for sample illumination [18,19]. Although heating of the samples due to the high intensity illumination employed was not reported in these studies, Polyakov *et al.* have previously shown that high-powered illumination of Ge nanowires can have a detrimental effect on their photoconductivity by causing exponential thermo-generated current increase inside them[8]. In our study, low-power illumination of 1-4 $\mu W \cdot cm^{-2}$ was used to study the optoelectronic response of Bi_2S_3 nanowires as a function of illuminating light photon energy, minimizing any effects due to sample heating and illustrating high optical sensitivity of the nanowires.

II. METHODS

A. Synthesis.

Highly-oriented single crystal Bi_2S_3 nanowires were synthesized inside the pores of AAO membranes using a solventless approach as previously described by Xu *et al.* [21]. The nominal diameter of the AAO pores was 200 nm. Scanning electron microscopy (SEM) images of the top and side views of a porous AAO membrane filled with Bi_2S_3 nanowires are shown in Figure 1.

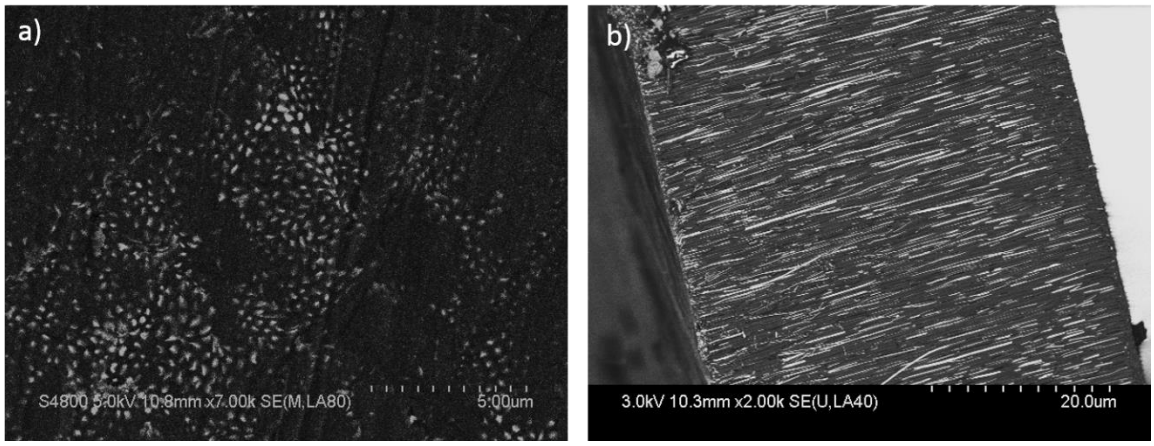

FIG. 1. SEM images of AAO templates filled with Bi_2S_3 nanowires (bright spots): (a) top view and (b) side view.

The total pore filling ratio, calculated from the SEM images, was up to 80 % with a maximum density of 8×10^8 nanowires per cm^2. The high yield of pore filling was achieved by injecting the melted single source precursor (bismuth bis(diethyldithiocarbamate) $[Bi(S_2CNEt_2)_3]$ into the AAO pores followed by thermolysis.

B. Sample Preparation.

Individual Bi_2S_3 nanowires were released from AAO membranes by dissolving the membranes in 9 % phosphoric acid. The liberated nanowires were subsequently sonicated in dichloroethane for 2 min and spin-coated onto a silica-coated Si substrate. Electron beam lithography (Raith ELPHY Quantum) and metallization (Gatan PECS 682 system) were used to make contacts (5 nm Ti/150 nm Au) to selected nanowires. Contacts to individual Bi_2S_3 nanowires are shown in the SEM image in Figure 2(a). A Hitachi S-4800 SEM was used for sample inspection. The nanowire illumination for photoconductive measurements occurred normal to the nanowire axis.

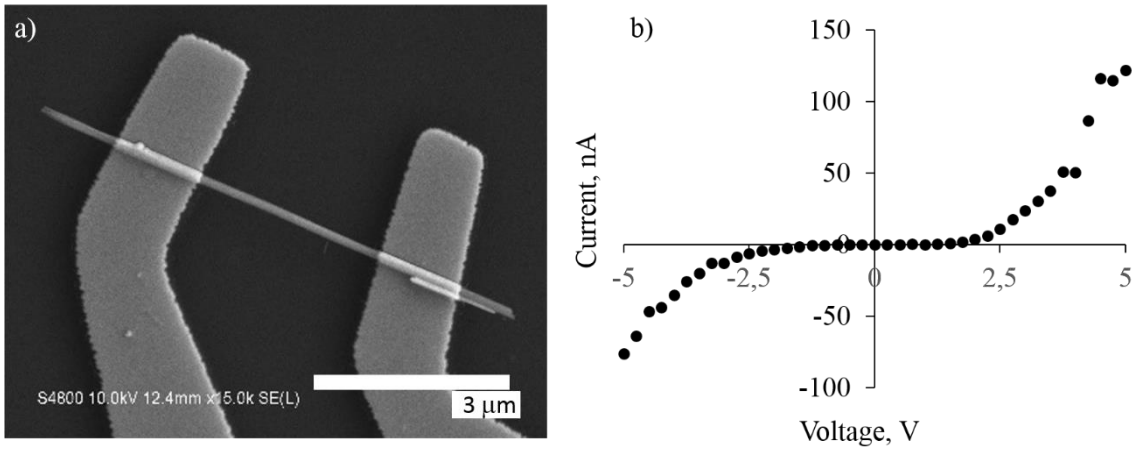

FIG. 2. (a) SEM image of a SiO_2-coated Si substrate showing deposited Bi_2S_3 nanowires (diameters around 200 nm) and Ti/Au electrodes. (b) Typical current-voltage characteristics of an individual Bi_2S_3 nanowire released from the AAO membrane.

For the comparison with the individual nanowires, as-produced arrays of Bi_2S_3 nanowires within the AAO membranes were prepared for photoconductive characterization by mechanically polishing both sides of the membranes, using ultra-fine sandpapers with grain sizes ranging from 12.6 to 8.4 μm (ISO P1500-2500), followed by polishing with a water-based diamond suspension, with grain sizes between 6 μm to 50 nm. After polishing, the thickness of the AAO membrane and respectively lengths of the nanowires were 40 μm and 5 μm. For the measurements, electrodes were deposited onto the polished samples. The top side of the samples was covered with a 15-20 nm gold layer which served as a semi-transparent conductive electrode. A macroelectrode, formed from a 40 nm thick gold layer, was deposited on the bottom side of the samples. A schematic of the experimental setup is shown in Figure 3(a). The light source for photoconductivity measurements was located in two different positions (Figure 3(a)). Positions 1 and 2 of the light source provided sample illumination along the nanowire axis and normal to the nanowire axis respectively.

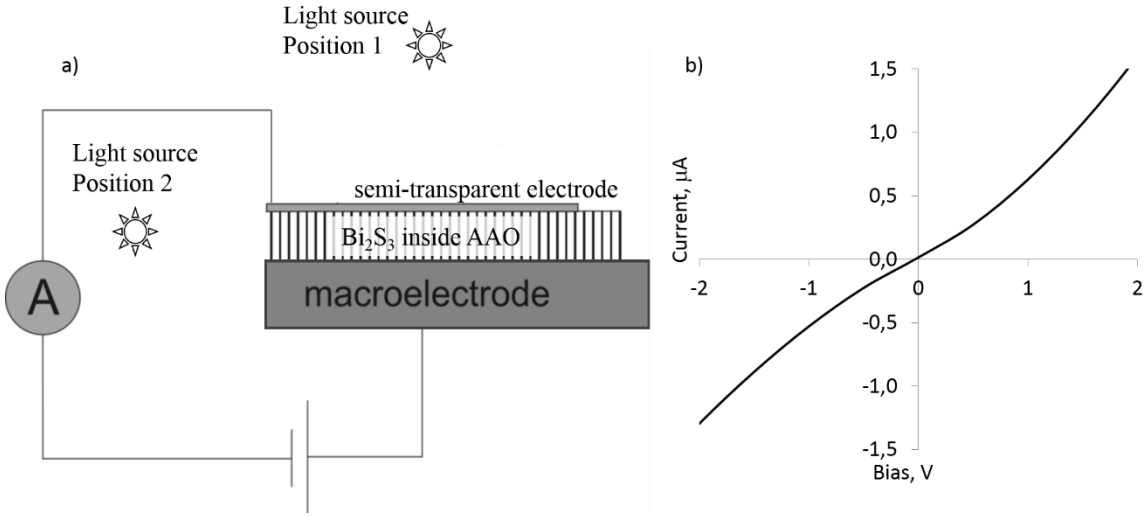

FIG. 3. (a) Schematic showing the experimental set-up for measuring the photoconductive properties of AAO-hosted Bi_2S_3 nanowires. The light source was located in Position 1 for the sample illumination along the nanowire axis or in the Position 2 for the sample illumination normal to the nanowire axis; (b) typical current-voltage characteristics obtained from an array of Bi_2S_3 nanowires within an AAO membrane.

A Keithley-6430 picoammeter was used for current-voltage characteristic measurements and photocurrent response (with step 0.625 s). Current-voltage characteristics of individual and arrays of Bi_2S_3 nanowires within AAO membranes were measured in the dark to assess the quality of nanowire/electrode contacts. Typical current-voltage 'dark' characteristics are shown in the Figure 2(b) for an individual nanowire and in the Figure 3(b) for nanowires hosted inside an AAO membrane. The I-V characteristics of the both individual and AAO-hosted Bi_2S_3 nanowires exhibit non-linear I-V characteristic, similar to those measured by Birjukovs et al. by conducting atomic force microscopy method[22], indicating the partial contribution of contact resistance. Due to the "non-conductive" gap caused by the contact resistance in the case of the individual nanowire, its photoconductivity spectra as a function of illuminating photon energy was measured at a bias of 5 V applied to the nanowire. The photoconductivity spectra of AAO-hosted nanowires were measured at constant bias of 1V applied to the sample.

For the low-power illumination of the samples, light from a tungsten filament lamp was passed through a system consisting of a diffraction grating, prisms and mirrors resulting in a spectrum with wavelengths between 500 - 900 nm with step of 5-10 nm at constant intensities 1-4 $\mu W \cdot cm^{-2}$, which are the minimal intensity values that could cause detectable photocurrent in the samples. The intensity of the illuminating light was measured with a Newport Optical Power Meter 1928-C. An Ocean Optics USB minispectrometer was used for the wavelength registration. All measurements were carried out at the room temperature in open air conditions.

III. RESULTS AND DISCUSSION

A. Photoconductivity spectra.

The maximal photocurrent signal could be obtained when illuminated area of the nanowire is maximal. This requirement and electrode placement opportunities determine the configuration of the experimental setup for the photoconductivity measurements. For the individual nanowire placed onto the substrate (Figure 2 (a)) the maximal impact of the illumination was achieved by location of the light source above the substrate so the nanowire was illuminated normal to its axis simultaneously along all its length.

For the nanowire arrays hosted inside an AAO template, the maximal possible number of the nanowires should be connected into the electrical circuit and illuminated. This was achieved by deposition of the semi-transparent electrode with diameter of 2 mm (which covered approx. 10^6 nanowires) onto the top surface of the polished AAO template filled with Bi_2S_3 nanowires (Figure 3 (a)). To illuminate all connected to the semi-transparent electrode nanowires, the AAO template was illuminated from Position 1 (Figure 3 a).

Figure 4 illustrates measured and normalized photoconductivity spectra of an individual Bi_2S_3 nanowire and AAO-hosted Bi_2S_3 nanowires.

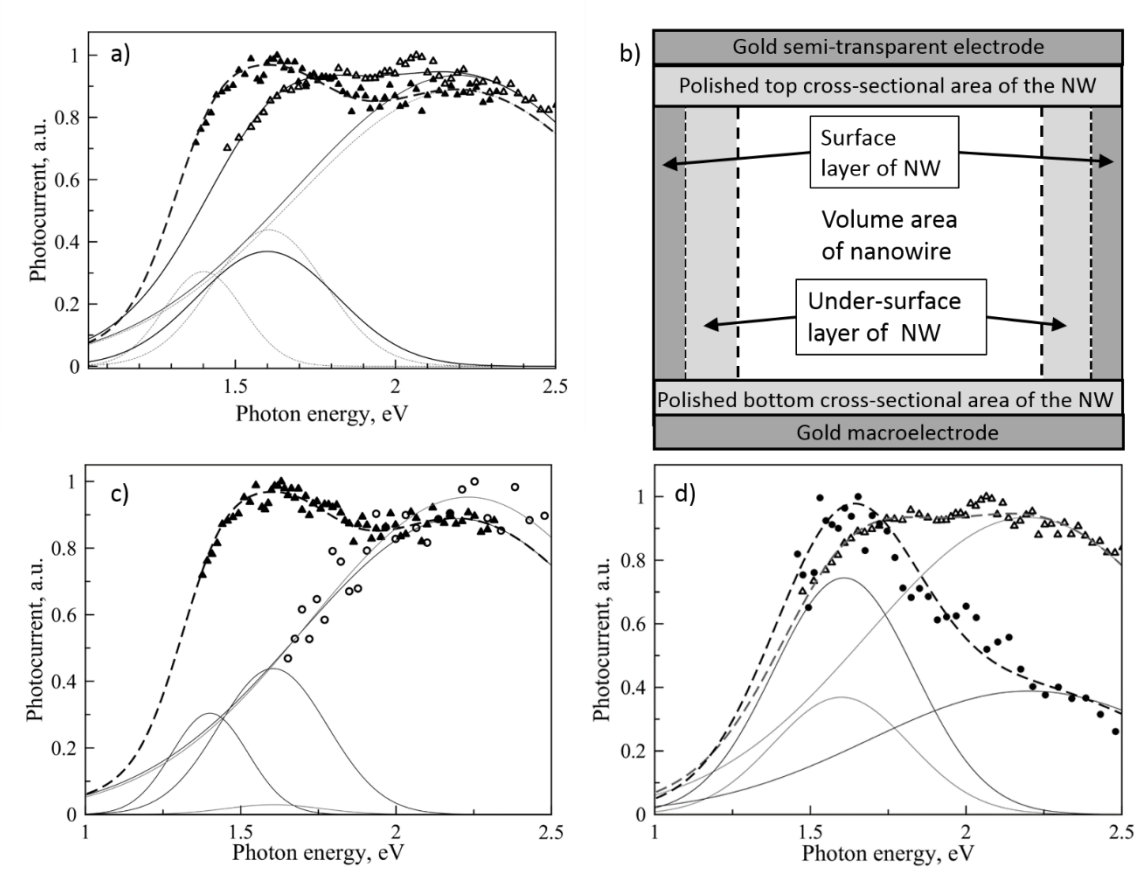

FIG. 4. Characterization of photoconductivity of Bi_2S_3 nanowires. (a) photoconductivity spectra of an individual Bi_2S_3 nanowire deposited onto a Si substrate (filled triangles) and of arrays of 40 μm long AAO-hosted Bi_2S_3 nanowires (not filled triangles) illuminated from Position 1 (Figure 3 a) ; (b) schematics of the nanowire areas with different charge carrier photo-induction energies; (c) photoconductivity spectra of the individual Bi_2S_3 nanowire deposited onto a Si substrate (filled triangles) and of AAO-hosted 40 μm long nanowires arrays (not filled circles) illuminated from Position 2 (Figure 3 a); d) photoconductivity spectra of AAO-hosted 40 μm long nanowires arrays (triangles) and of AAO-hosted 5 μm long nanowires arrays (circles) illuminated from Position 1 (Figure 3 a).

Deconvolution of the measured spectra of the individual nanowire and 40 μm long AAO- hosted nanowires into the energy peaks (Figure 4 a) resulted in three energy peaks for the spectrum of the individual nanowire and in two energy peaks for the spectrum of AAO-hosted nanowires. Maxima of these energy peaks were located at 1.4 eV, 1.6 eV and 2.2 eV for the individual nanowire and at 1.6 eV and 2.2 eV for the AAO-hosted nanowires. We presume that these energy peaks are related to the photo-inducing of the charge carriers in different areas of nanowire (see schematic image in Figure 4 b). Energy peaks of nearly the same heights with maxima located at 2.2.eV were presented in spectra of both the individual and AAO-hosted nanowires and correlated well with the photoconductivity spectrum reported for Bi_2S_3 thin films[16]. Thus, these peaks could be attributed to the photo-induced in the nanowires' volume (Figure 4 b) charge carriers.

The energy peak with maximum located at 1.4 eV, which was presented only in the spectrum of the individual nanowire liberated from the AAO template, but not in the spectrum of the AAO-hosted nanowires, could be attributed to the inducing of the charge carriers on the surface of the nanowire where sub-band gap energy levels could be presented as a result

of high density of defects caused by the environmental impact on the nanowire's surface. The AAO-hosted nanowires did not show any energy peaks at the energies lower than 1.6 eV. We suggested that in this case the photo-induced on the surface of nanowires charge carriers were trapped by the surrounding AAO and could no longer contribute to the photoconductivity. Similar effect was previously reported by *Kouklin et al*. [23], who suggested that the wave functions of electrons in the AAO-templated semiconductor (CdS) nanowires penetrate a short distance into the surrounding alumina as a result of photo-assisted process, where electrons get trapped at the sub-band energy levels and can no longer contribute to conduction.

Energy peaks with maxima located at 1.6 eV could be attributed to the charge carriers induced in the under-surface areas of the nanowires (Figure 4 b). Contribution of these charge carriers to the conductance of the nanowires may be significant gratefully to the high surface-to-volume ratio of the nanowires. For the AAO-hosted nanowires, we suggested that this energy peak was related not only with photo-induced in the under-surface areas of the nanowires charge carriers, but also with the charge carriers induced in the mechanically polished top and bottom cross-sectional areas of the nanowires and in the nanowire/gold interface. The photon energy required to induce the charge carriers in the under-surface layer of nanowires may be lower in comparison with the energy necessary to induce volume charge carriers in the nanowires due to the higher density of defects formed under the influence of the surface structure.

To clarify the role of the AAO in the nanowires conductance, spectrum of the 40 μm long AAO hosted nanowires illuminated from Position 2 (Figure 3 a) was measured and compared with the spectrum measured for the individual nanowire. For the AAO - hosted nanowires, the illumination from Position 2 is not optimal for the achievement of the maximal photocurrent signal of the nanowires because in the illuminated from side AAO template the nanowires located deeper inside the template were partially or fully shielded from the impact of the illuminating light and could give only partial or no contribution to the photocurrent, but just to the background current, thus complicating evaluation of the photoconductivity of the sample. Nevertheless, measurements in this configuration were important for understanding of a mechanism of photoconductivity of AAO-hosted nanowire arrays because contribution of the photo-induced in the polished top and bottom cross-section areas and in the gold/nanowire interface charge carriers to the nanowire conductance was minimised thus highlighting the behaviour of the nanowire/AAO interface.

Comparison between the spectra of the individual Bi_2S_3 nanowire and AAO-hosted nanowires illuminated from the Position 2 (Figure 3 a) is shown in the Figure 4 c. In contradiction with the spectrum for the individual nanowire were energy peaks with maxima at 1.4, 1.6 and 2.2 eV were presented (Figure 4 a,c (filled triangles)), deconvolution of the spectrum of the AAO-hosted nanowires (Figure 4 c, circles) into energy peaks resulted in two peaks with maxima located at 1.6 and 2.2 eV. Whilst heights of the 2.2 eV energy peaks were nearly the same for both spectra, the height of the 1.6 eV energy peak of

the spectrum of the AAO-hosted nanowires was by the order of magnitude smaller than peak of the same energy of the individual nanowire spectrum, but peak at 1.4 eV, by our suggestion related to the charge carriers induced onto the surface of the nanowire, was not presented at all. This proves the hypothesis that the surrounding AAO traps most of the photo-induced on the nanowires surface charge carriers as well as most of the charge carriers induced into the under-surface areas of the nanowires. Thus, when the nanowires were illuminated from side, the significant due to the high surface-to-volume ratio of the nanowire contribution of the induced on the surface and into the under-surface areas along all the individual nanowire charge carriers resulted in its photoconductivity spectrum with pronounced local maximum located at approx 1.6 eV (Figure 4 a, c (filled triangles)). In the AAO-hosted nanowires illuminated from top, the photoconductivity was determined mostly by the photo-induced in the volume of the nanowires charge carriers as well as by the charge carriers photo-induced in the polished top and bottom cross-section areas of the nanowires and in the nanowire/gold interface.

Significant contribution of the photo-induced in the polished top and bottom cross section areas of the nanowires and in the nanowire/gold interface was proved also by comparison of photoconductivity spectra of 5 and 40 μm thick AAO template filled with Bi_2S_3 nanowires illuminated from the Position 1 (Figure 3 a, Figure 4 d). Similarly to the 40 μm nanowires, deconvolution of the spectrum of the 5 μm long nanowires resulted in two energy peaks with maxima located at 1.6 and 2.2 eV. Absence of the energy peaks at energies lower than 1.6 eV proved the hypothesis that most of the induced on the nanowires' surfaces charge carriers were trapped by the surrounding alumina and eliminated from the conductance. At the same time, energy peaks at 1.6 eV had height ratio approx 2:1 and the energy peaks at 2.2 eV had height ratio approx 1:2.25 (5 μm long nanowires (Figure 4 d, circles) vs 40 μm long nanowires (Figure 4 d, triangles)), so in the case of 5μm long nanowires the energy peak at 1.6eV was dominating over the energy peak at 2.2 eV. The difference in the peaks heights could be explained as following: during the illumination of the nanowires from the Position 1, the light beam was travelling along the nanowire's axis inducing the charge carriers. The most of the charge carriers induced in the under-surface areas of the nanowires were trapped by the surrounding AAO. Contribution of the charge carriers induced in the polished top and bottom cross-section areas of the short nanowires and in the nanowire/gold interface (energy peak at 1.6 eV) to the conductance was twice larger in comparison to the long nanowires due to the short travel distance along the nanowire. There was smaller chance for the induced charge carriers to move to the nanowire's surface and to get eliminated from the conductance by the traps in surrounding AAO or to recombine before reaching the counter electrode.

These measurements also proved that the compared in the Figure 4 a spectra of the individual Bi_2S_3 nanowire and AAO-hosted 40 μm long Bi_2S_3 nanowires were determined not by the different geometrical orientation of the nanowires

relative to the illuminating light beam, but were the result of superposition of contribution of the photo-induced in different areas of the nanowire charge carriers to the conductance plus the impact of the AAO that surrounding the nanowires.

B. Determination of photoresponse values and kinetics.

For the determination of the ability of liberated from AAO membrane individual Bi_2S_3 nanowires to serve as an active elements of an optical device at low illumination levels, their photoresponse value was determined and compared with this of arrays of AAO-hosted nanowires. An increase and decay in the photocurrent relatively to the dark current were measured (Figure 5 a) at photon energies corresponding to the most pronounced maxima of the photoconductivity spectra.

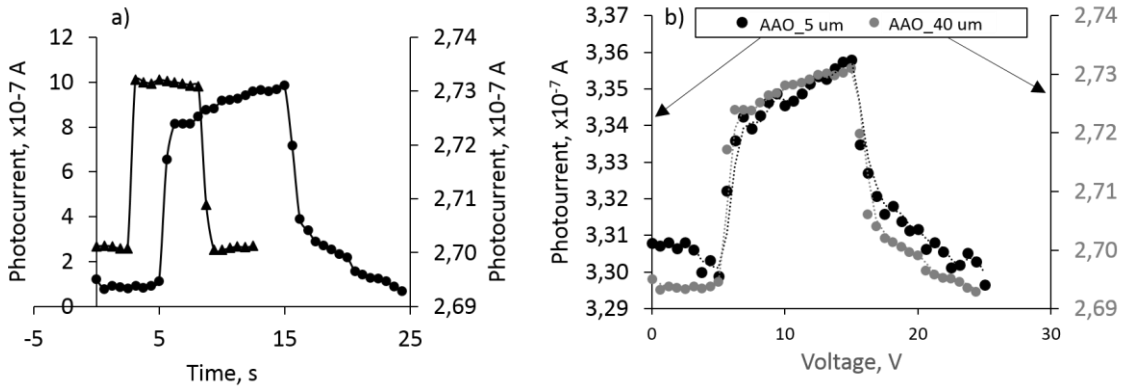

FIG. 5. (a) Photocurrent vs time for plots for individual (triangles) and AAO-hosted (circles) Bi_2S_3 nanowires; (b) comparison between photocurrent impulses of 5μm long (black circles) and 40 μm long (grey circles) AAO-hosted Bi_2S_3 nanowires.

For the illuminating photon energy of 1.6 eV, the individual Bi_2S_3 nanowire displayed rapid one-step increase in photocurrent by 80 %/V relative to the dark current (Figure 5 a, triangles) at the moment when the illumination was turned on, followed by photocurrent stabilisation during the further illumination. After the illumination light was turned off, the individual Bi_2S_3 nanowire showed immediate photocurrent drop down to the dark current level. Such reaction on low-power illumination makes the liberated from AAO membrane Bi_2S_3 nanowires promising candidates for the use in low-power optical devices. In contradiction, the AAO-hosted nanowires displayed slightly slower increase in photocurrent (Figure 5 a, circles) just by 1%/V at the moment when the illumination with photon energy of 2.2 eV was turned on. The photocurrent was continuously increasing during the illumination time. After the illumination was turned off, the AAO-hosted nanowires displayed rapid photocurrent drop by approx. 60% followed by slow (>8 s) photocurrent decrease down to the dark current level (Figure 5 a, circles). To clarify the reasons for described photocurrent kinetics, the photocurrent impulses for Bi_2S_3-filled AAO templates with thicknesses 5 μm and 40 μm were compared (Figure 5 b). As it is seen from this Figure, there was no significant difference in the photocurrent kinetics. This proves that the reason for continuous photocurrent increase during

the illumination as well as slower photocurrent onset/decay times was not a photo-induced carrier concentration gradient along the length of the nanowires which could require a longer time to saturate/recombine. We suggested that probably the relatively slow increase of photocurrent during the illumination and its slow decay after the illumination was turned off could be related to a gradual release of trapped in trap energy levels at the nanowire/AAO interface charge carriers. This question is not immediately clear and needs further investigation. At this moment, minor increase in photocurrent and large inertia of optical response hinder the use of as-produced AAO-hosted Bi_2S_3 nanowire arrays in low-power optical devices. Potentially, the impact of the AAO/nanowire interface on the photoconductive properties of the Bi_2S_3 nanowires may be significantly reduced by pre-treatment of the AAO membrane pore inner surfaces prior the nanowire synthesis (for example, as reported by Xiong et al[24], atomic layer deposition (ALD) coating of AAO membranes by Al_2O_3 both forms a compositionally uniform surface and modifies the types of hydroxyl groups present on the AAO pore inner surface) and introducing defects into the surfaces of AAO-hosted nanowires.

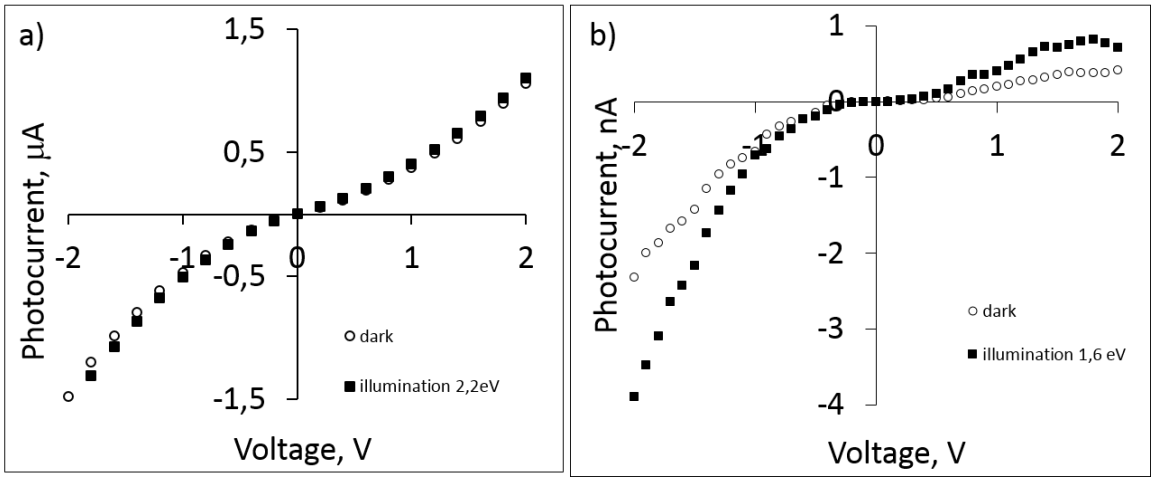

FIG. 6. Comparison between dark (circles) and illuminated (squares) current-voltage characteristics of AAO-hosted (a) and individual (b) Bi_2S_3 nanowires.

The difference in the photocurrent response values and photocurrent onset/decay time between the individual Bi_2S_3 nanowire liberated from the AAO membrane and the AAO-hosted nanowires was probably due to the impact of the AAO template surrounding the nanowires was also proved by the comparison of the current-voltage curves of the samples, measured in darkness and under illumination (Figure 6). There was minor (up to 5%) difference between the I-V curves of the AAO-Bi_2S_3 sample (Figure 6 (a)), while the I-V curves of the individual nanowire (Figure 6 (b)) exhibited noticeable (up to 50 %) increase in current under the illumination. These measurements allowed to suggest that in the AAO-hosted nanowires the most of the photo-induced charge carriers were deprived of the opportunity to contribute to the conductance by the surrounding alumina.

IV. CONCLUSIONS

Photoconductive properties of liberated from the AAO membrane individual Bi_2S_3 nanowires were investigated under low-intensity illumination and compared with properties of as-produced AAO-hosted Bi_2S_3 nanowire arrays. On the basis of the experimental results it was suggested that photoconductivity spectra were result of superposition of photo-induced in different areas of the nanowires charge carriers. Also, it was suggested that the AAO template deprives significant part of the photo-induced on the surface and in the under-surface areas of the nanowires charge carriers of the opportunity to contribute to the nanowires conductance.

The individual Bi_2S_3 nanowires showed fast and pronounced – 80%/V – photoresponse and small inertia of optical reaction development under low-power illumination, which makes these nanowires promising candidates for use in low-power optical devices as active elements. In contradiction to the individual Bi_2S_3 nanowire, AAO-hosted nanowire arrays exhibited slight photocurrent increase in combination with longer photocurrent rise and decay times and large optical reaction inertia, making it difficult to use as-produced AAO-hosted hosted Bi_2S_3 nanowire arrays in low-power optical devices. Such a difference in photoconductive properties between the individual nanowire and the AAO-hosted nanowires proved the hypothesis about the presence of charge carrier trap levels in the alumina template surrounding the nanowires preventing the photo-induced in the nanowires charge carriers from the contribution to the nanowire conductance.

ACKNOWLEDGEMENTS

This work is supported by Latvia National program in Materials Science and by Science Foundation Ireland (SFI) under the FORME Strategic Research Cluster Award (Project 07/SRC/I1172). Authors thank Dr. Juris Prikulis for assistance in experiments and valuable discussions.

REFERENCES

[1] J. F. Wang, M. S. Gudiksen, X. F. Duan, Y. Cui and C. M. Lieber, Science **293,** 1455 **(**2001).

[2] Y. Cui, Q. Q. Wei, H. K. Park and C. M. Lieber, Science **293**, 1289 (2001).

[3] Y. Huang, X. F. Duan, Q. Q. Wei and C. M. Lieber, Science **291**, 630 (2001).

[4] Y. N. Xia, P. D. Yang, Y. G. Sun, Y. Y. Wu, B. Mayers, B. Gates, Y. D. Yin, F. Kim and Y. Q. Yan, Adv. Mater. **15**, 353 (2003).

[5] Z. W. Pan, Z. R. Dai and Z. L. Wang, Science **291**, 1947 (2001).

[6] H. Kind, H. Q. Yan, B. Messer, M. Law and P. D. Yang, Adv. Mater. **14**, 158 (2002).

[7] X. Wu, J. S. Kulkarni, G. Collins, N. Petkov, D. E. Almécija, J. J. Boland, D. Erts and J. D. Holmes, Chem. Mater. **20**, 5954 (2008).

[8] B. Polyakov, B. Daly, J. Prikulis, V. Lisauskas, B. Vengalis, M. Morris, J. D. Holmes and D. Erts, Adv. Mater. **18**, 1812 (2006).

[9] C. Soci, A. Zhang, X.-Y. Bao, H. Kim, Y. Lo, and D. J. Wang, Nanosci. Nanotechnol. **10**, 1430 (2010).

[10] R. R. LaPierre, A. C. E. Chia, S. J. Gibson, C. M. Haapamaki, J. Boulanger, R. Yee, P. Kuyanov, J. Zhang, N. Tajik, N. Jewell and K. M. A. Rahman, Phys. Status Solidi RRL **7**, 815 (2013).

[11] D. J. Sirbuly, M. Law, P. Pauzauskie, H. Yan, A. V. Maslov, K. Knutsen, C.-Z. Ning, R. J. Saykally and P. Yang, PNAS **102**, 7800 (2005).

[12] H. Bao, X. Cui, C. M. Li, Y. Gan, J. Zhang and J. Guo, J. Phys. Chem. C **111**, 12279 (2007).

[13] H. Bao, C. M. Li, X. Cui, Q. Song, H. Yang and J. Guo, Nanotechnology **19**, 335302 (2008).

[14] J. Wang and M. Isshiki, Springer Handbook of Electronic and Photonic Materials, 325 (2007).

[15] J. D. Klein, R. D. Herrick, D. Palmer and M. J. Sailor, J. Chem. Mater. **5**, 902 (1993).

[16] Z. Kebbab, N. Benramdane, M. Medles, A. Bouzidi and H. Tabet-Derraz, Sol. Energy Mater. Sol. Cells **71**, 449 (2002).

[17] S. Mahmoud, A. H. Eid and H. Omar, FIZIKA A 6 **3**, 111 (1997).

[18] A. A. Tahir, M. A. Ehsan, M. Mazhar, K. G. Wijayantha, M. Zeller and A. D. Hunter, Chem. Mater. **22**, 5084 (2010).

[19] R. S. Mane, B. R. Sankapal and C. D. Lokhande, Mater. Chem. and Phys. **6**, 196 (1999).

[20] Y. Xi, C. Hu, X. Zhang, Y. Zhang and Z. L. Wang, Solid State Commun. **149**, 1894 (2009).

[21] J. Xu, N. Petkov, X. Wu, D. Iacopino, A. J. Quinn, G. Redmond, T. Bein, M. A. Morris and J, D. Holmes, ChemPhysChem **8**, 23 (2007).

[22] P. Birjukovs, N. Petkov, J. Xu, J. Svirksts, J. J. Boland, J. D. Holmes and D. Erts, J. Phys. Chem. C **112**, 19680 (2008).

[23] N. Kouklin, L. Menon, A. Z. Wong, D. W. Thompson, J. A. Woollam, P. F. Williams and S.Bandyopadhyay, Appl. Phys. Lett 79, 4423 (2001).

[24] G. Xiong, J. W. Elam, H. Feng, C. Y. Han, H.-H. Wang, L. E. Iton, L. A. Curtiss, M. J. Pellin, M. Kung, H. Kung and P. C. Stair, J. Phys. Chem. **109**, 14059 (2005).